Two-step high-pressure high-temperature synthesis of nanodiamonds from naphthalene*

Tong Liu(刘童), Xi-Gui Yang(杨西贵)†, Zhen Li(李振), Yan-Wei Hu(胡宴伟), Chao-Fan Lv(吕超凡), Wen-Bo Zhao(赵文博), Jin-Hao Zang(臧金浩)‡, and Chong-Xin Shan(单崇新)§

Henan Key Laboratory of Diamond Optoelectronic Materials and Devices, Key Laboratory of Materials Physics, Ministry of Education, School of Physics and Microelectronics, Zhengzhou University, Zhengzhou 450052, *China*

(Received 25 July 2020; revised manuscript received 3 August 2020; accepted manuscript online 7 August 2020)

Nanodiamonds have outstanding mechanical properties, chemical inertness, and biocompatibility, which give them potential in various applications. Current methods for preparing nanodiamonds often lead to products with impurities and uneven morphologies. We report a two-step high-pressure high-temperature (HPHT) method to synthesize nanodiamonds using naphthalene as the precursor without metal catalysts. The grain size of the diamonds decreases with increasing carbonization time (at constant pressure and temperature of 11.5 GPa and 700 °C, respectively). This is discussed in terms of the different crystallinities of the carbon intermediates. The probability of secondary anvil cracking during the HPHT process is also reduced. These results indicate that the two-step method is efficient for synthesizing nanodiamonds, and that it is applicable to other organic precursors.

Keywords: nanodiamonds, high pressure high temperature, phase transition, naphthalene

PACS: 81.05.ug, 62.50.−p, 64.70.Nd, 07.35.+k **DOI:** 10.1088/1674-1056/abad1c

1. Introduction

Nanodiamonds have outstanding mechanical[1–3] and optical properties,[4] high biocompatibility, low toxicity, and large surface area.[5] These factors make nanodiamonds promising candidates in applications such as fine grinding and polishing,[6,7] single photon emitters in quantum optics,[8,9] luminescent hybrid materials,[10,11] drug delivery, and bioimaging.[12–19]

The most common large-scale methods for preparing nanodiamonds are detonation synthesis and the high-pressure high-temperature (HPHT) technique,[20,21] both of which have limitations. In detonation synthesis, the nanodiamonds usually have high contents of impurities and require tedious purification which is costly and detrimental to the environment.[22,23] In the traditional HPHT technique, metals are often used as catalysts which can allow for more mild synthesis conditions, but inevitably introduces impurities. Nanodiamond particles prepared in this method usually have sharp edges and haphazard shapes resembling those of broken glass.[24,25] The low purity and uneven morphology of the synthesized nanodiamonds currently restrict their applications.

In recent years, organic species have been employed as precursors for the HPHT synthesis of nanodiamonds without metal catalysts. For instance, nanodiamonds were synthesized from adamantane in titanium tubes at about 9 GPa and 1267 ℃.[26] Carbon samples containing 30–50 nm-sized diamond nanoparticles were synthesized using adipic acid ($C_6H_{10}O_4$) as a precursor at 14 GPa and 1235 ℃.[27] Coexisting micron- and nano-sized diamonds were formed through thermal transformations of binary mixtures of naphthalene and octafluoronaphthalene at 8 GPa and 1500 ℃. The large amounts of nano-sized diamonds were attributed to the specifics of carbonization of the fluorocarbons under pressure.[28] Sub-micron-sized diamonds containing a small number of nanodiamond particles were synthesized from naphthalene at 11 GPa and 1700 ℃ without using metal catalysts.[29] These methods afforded high-purity nanodiamonds without the use of metal catalysts. However, significant hydrogen, methane, or ethane are produced under the HPHT conditions when using organics as precursors.[30,31] This leads to drastic volume shrinkage which often damages the secondary anvil and chamber of the HPHT apparatus (6–8 multi-anvil apparatus), thus hindering the application of organic precursors in the HPHT process.

In this work, we report a two-step HPHT method for synthesizing nanodiamonds from a naphthalene precursor. This method includes a carbonization step at 11.5 GPa and 700 ℃ and a subsequent diamondation step at 11.5 GPa and 1700 ℃. The grain size of the diamonds can be tuned by varying the carbonization time. This method also reduces the probability of secondary anvil cracking in the HPHT process.

*Project supported by the National Key R&D Program of China (Grant No. 2018YFB0406500), the National Natural Science Foundation of China (Grant Nos. U1804155, U1604263, and 11804307), and the China Postdoctoral Science Foundation (Grant Nos. 2018M630830 and 2019T120631).

†Corresponding author. E-mail: yangxg@zzu.edu.cn

‡Corresponding author. E-mail: jinhao_zang@zzu.edu.cn

§Corresponding author. E-mail: cxshan@zzu.edu.cn

2. Experimental details

Naphthalene (Shanghai Macklin Biochemical Co., Ltd.) was used as the precursor without further purification. The synthesis was carried out in a Kawai/Walker type multi anvil apparatus.[32] The experiment mainly adopted the 14/8 (G2) assembly reported by Leinenweber *et al.*[33]

Cylindrical samples of the naphthalene precursor (3.5 mm in diameter and 2.8 mm in height) were first obtained by cold compression. The pressed samples were placed in a graphite container, which was also used as the heater for the HPHT apparatus. The phase transition from organic naphthalene to diamond under HPHT conditions was accomplished in a closed environment. Detailed experimental steps are shown in Fig. S1 of supplementary material.

The experimental procedure initially involved increasing the pressure in the apparatus to 11.5 GPa at room temperature. As shown in Scheme 1, the temperature rise occurred in two steps. In step 1, the precursor was slowly heated to 700 ℃ (heating rate of 2 ℃ per second) for 35 min, 90 min, 135 min, and 180 min, respectively. Carbon intermediates with different crystallinities were obtained, thus it is referred to as the carbonization step. In step 2, the carbon intermediates with different crystallinities were heated to 1700 ℃ (heating rate of 25 ℃ per second), at which the temperature was maintained for 5 min. The intermediates were converted into diamonds, thus it is referred to as the diamondation step. Finally, the samples were cooled to ambient conditions, purified with acid and dried.

The resulting samples were labeled N1, N2, N3, and N4, for carbonization time of 35 min, 90 min, 135 min, and 180 min, respectively. For comparison, samples NX (X = 5–8) were also obtained at 11.5 GPa and 700 ℃ for carbonization time for 35 min, 90 min, 135 min, and 180 min, respectively, but without the subsequent diamondation step. The pressure was calibrated by the pressure-induced phase transitions of bismuth, barium, and thallium. The temperature was monitored using a W5%Re–W26%Re thermocouple (C-type). The measurement error throughout the temperature and pressure ranges was less than 5%.

The samples were analyzed at ambient conditions by x-ray diffraction (XRD), Raman spectroscopy, scanning electron microscopy (SEM), and transmission electron microscopy (TEM). XRD patterns were obtained using Cu K_α (0.154 nm) as the radiation source (Rigaku, SmartLab). Raman measurements were carried out using a SOL spectrometer (Confotec, MR520) equipped with a 532 nm wavelength laser. SEM images were collected using a JSM-6700 F apparatus (JEOL, Japan). TEM images were collected using an FEOL-2010 microscope (Japan) operated at 200 kV.

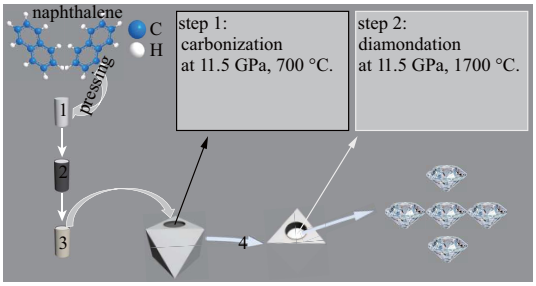

Scheme 1. Schematic of the synthesis of nanodiamonds via the two-step HPHT method. 1. cylindrical sample of the precursor naphthalene; 2. graphite container; 3. ZrO_2 sleeve; 4. octahedron pressure medium of MgO.

3. Results and discussion

Figure 1 shows the XRD patterns and Raman spectra of samples NX (X = 1–4). The XRD patterns are used to determine the composition.[34] Figure 1(a) shows that three dominant peaks at around 43.8°, 75.3°, and 91.4° are observed in the XRD patterns of samples NX (X = 1–4), which are attributed to diffractions from the (111), (220), and (311) planes of diamond, respectively. The XRD patterns of samples NX (X = 1–4) also exhibit two weak peaks from the (002) and (100) planes of graphite, indicating that some graphite is not converted to diamond. Figure S2 shows the EDS spectra of samples NX (X = 1–4). The percentage of carbon in samples NX (X = 1–4) is higher than 95%, which indicates that they are all of high purity.[35] Raman spectroscopy is used to confirm the formation of diamond, as shown in Fig. 1(b). The spectrum of naphthalene exhibits two peaks at around 1382 cm^{-1} and 1576 cm^{-1} which are assigned to the totally symmetric vibrations $\nu_5(a_g)$ and $\nu_3(a_g)$, respectively.[36] Samples NX (X = 1–4) all show the characteristic peak of diamond at 1332 cm^{-1}.

Table 1. The experimental conditions and results for samples NX (X = 1–8).

	Step 1: Carbonization at 11.5 GPa and 700 ℃		Step 2: Diamondation at 11.5 GPa and 1700 ℃	
	Time[a]/min	Morphology	Time[b]/s	Average size/nm
N1	35	/	300	457
N2	90	/	300	204
N3	135	/	300	62
N4	180	/	300	127
N5	35	amorphous	/	/
N6	90	chipped	/	/
N7	135	layered	/	/
N8	180	block	/	/

[a]Carbonization time; [b]constant temperature time at 11.5 GPa and 1700 ℃.

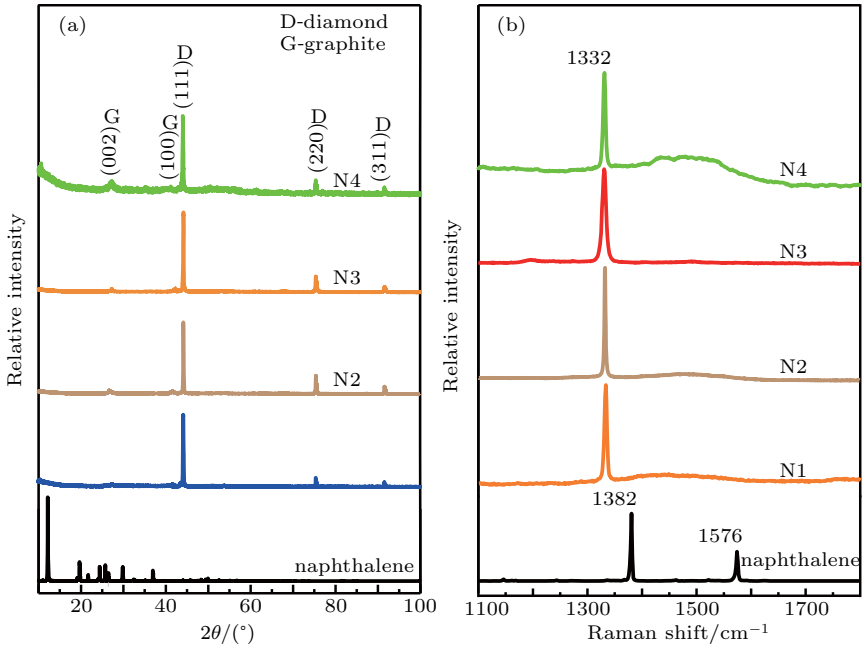

Fig. 1. (a) XRD patterns and (b) Raman spectra of the naphthalene precursor and samples NX (X = 1–4) prepared using different carbonization time at 11.5 GPa and 1700 °C.

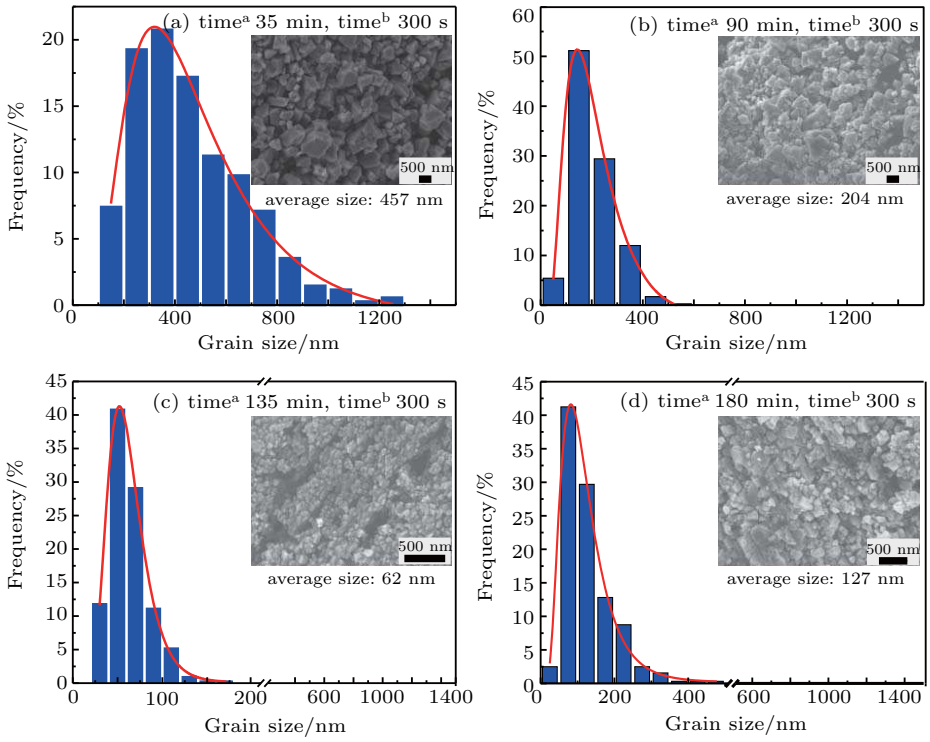

Fig. 2. (a)–(d) Grain size distributions of samples NX (X = 1–4) prepared using different carbonization time. The red curves show fitting of the lognormal distribution function. Inset shows the corresponding SEM images.

SEM images of samples NX (X = 1–4) synthesized with different carbonization time at 11.5 GPa and 1700 °C are shown in Fig. 2. These images show the typical morphologies of diamond particles with submicron and nanometre sizes. By measuring thousands of diamond particles in each image, the grain size distributions are obtained, as shown in Figs. 2(a)–2(d). The grain size in sample N1 is heterogeneous, while samples N2 and N3 have relatively homogeneous and smaller grain sizes. The average grain size of samples NX (X = 1–4) as a function of carbonization time is shown in Fig. 3. The average grain size decreases with increasing carbonization time, but suddenly increases when the carbonization time is increased to 180 min. This may be related to the carbon intermediates obtained during the carbonization process at different time. Figure S3 shows the XRD patterns of the naphthalene precursor and samples prepared at 11.5 GPa with different temperatures, from which the thermal transformation of naphthalene can be characterized. One can see that increasing the

temperature leads to the naphthalene precursor dehydrogenating to amorphous carbon, then to well-crystallized graphite, and finally to diamond when the temperature reaches 1700 ℃.

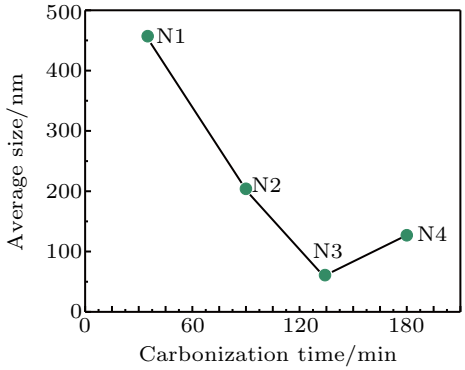

Fig. 3. Average grain size of samples NX (X = 1–4) as a function of carbonization time.

Figure 4 shows a TEM image and corresponding selected area electron diffraction pattern of sample N3. In Fig. 4(a), there are many nanodiamond grains with sizes of 40–120 nm. The HRTEM image in Fig. 4(a) inset shows well-resolved lattice fringes with a spacing of 0.206 nm, which corresponds to the (111) crystal plane of diamond.[37] The diffraction rings in Fig. 4(b) demonstrate the presence of nanodiamonds, corresponding to the (111), (220), and (311) planes in cubic diamond.

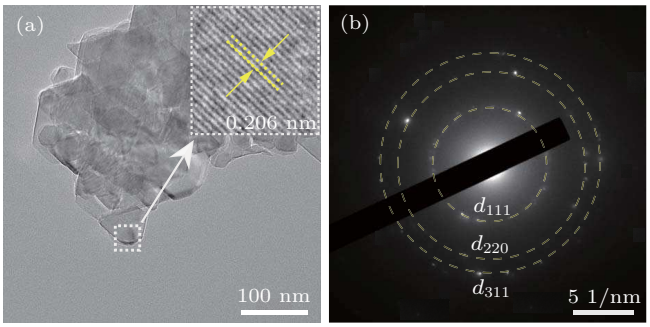

Fig. 4. (a) TEM image of sample N3. Inset shows HRTEM image of a single diamond particle from the white rectangle area marked in (a). (b) Selected area electron diffraction pattern of sample N3.

To explore the influence of carbonization products on the diamonds grain size, samples N5, N6, N7, and N8 were obtained at 11.5 GPa and 700 ℃ for carbonization time of 35 min, 90 min, 135 min, and 180 min, respectively. The mechanism of nucleation and growth of the synthesized diamond was studied by XRD, Raman spectroscopy, and SEM, as shown in Fig. 5. The XRD patterns in Fig. 5(a) show the different crystallinities of the samples. Sample N5 shows a typical XRD peak of amorphous carbon. The XRD pattern of sample N6 exhibits the (002) and two-dimensional (01) peaks characteristic of graphite. These two peaks at 23°–29° and 41°–47° are attributed to the stacking of parallel layer planes and the regular structure within the individual layer plane segments, respectively. Peaks of the type (hkl) are absent, indicating that sample N6 contains some disordered carbons.[38,39] Further increasing the carbonization time to 135 min or 180 min leads to the presence of the (100) peak for samples NX (X = 7, 8). This indicates the three-dimensional ordering of graphite planes and the beginning of graphite formation.

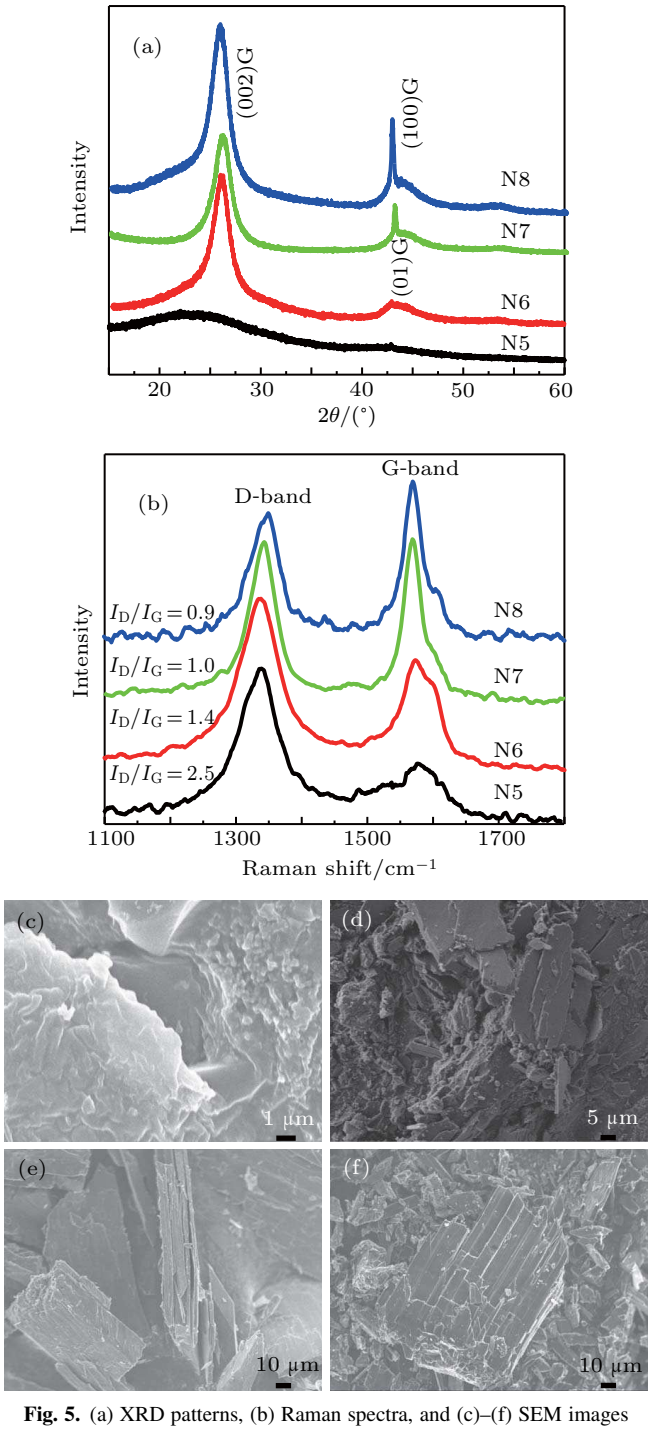

Fig. 5. (a) XRD patterns, (b) Raman spectra, and (c)–(f) SEM images of samples NX (X = 5–8) obtained using different carbonization time at 11.5 GPa and 700 ℃.

Graphite generally shows two characteristic Raman bands at 1350 cm^{-1} and 1580 cm^{-1}, which are the so-called D-band and G-band, respectively. The former is usually attributed to the A_{1g} breathing mode of carbon and is closely associated with lattice defects in graphite sheets. The latter is usually

attributed to the E_{2g} stretching mode of sp^2 bonded carbon. The D/G-band intensity ratio (I_D/I_G) directly reflects the degree of crystallinity and defects in the graphite.[40] As shown in Fig. 5(b), the values of I_D/I_G for samples N5–N8 gradually decrease from 2.5 to 0.9. This indicates that the crystallinity of graphite progressively increases with increasing carbonization time.

The SEM images in Figs. 5(c)–5(f) show carbon intermediates with different morphologies such as amorphous, chipped, layered, and block. Amorphous carbon is obtained at shorter carbonization time, while graphite is obtained and becomes gradually more ordered with increasing carbonization time. These observations are consistent with the results obtained from the XRD patterns and Raman spectra.

Carbonization is a necessary process in the transformation of hydrocarbon to diamond, which involves many complex reactions such as polymerization, poly-condensation, cracking reactions, molecular rearrangement, and hydrogen transfer.[41–45] Carbon intermediates with different crystallinities are obtained in samples NX (X = 5–8) by using different carbonization time at 11.5 GPa and 700 ℃. Their crystallinity increases with increasing carbonization time. It has been suggested that diamond nucleation is more likely to occur with carbon nanoparticles containing amorphous carbon as a precursor,[46–49] and that the quantity of nucleation and granularity of synthesized nanodiamonds decrease with increasing crystallinity of the graphite precursor.[50–53] Thus, the decreasing average grain size of samples N1–N3 with increasing carbonization time may be attributed to the increase of crystallinity of carbon intermediates, which does not favor the nucleation and growth of nanodiamonds. The average grain size of sample N4 is slightly larger than that of sample N3. Considering the higher crystallinity of the carbon intermediates in sample N8, the reason that the average grain size of sample N4 does not further decrease is probably related to the longer holding time which boosts the growth of nanodiamonds. It is reasonable to conclude that the change in grain size of samples NX (X = 1–4) is related to the effect of the corresponding carbon intermediates with different crystallinities obtained in the carbonization step. Note that in our present process, the naphthalene precursor is first converted into carbon intermediates by annealing at relatively low pressure and temperature. Therefore, the gases produced may be vented slowly during the process without damaging the equipment. The resulting graphitic materials are then heated to much higher temperatures for a few minutes to be converted into diamonds. In comparison with the commonly used detonation and metal-catalyst methods, the two-step HPHT method is more friendly to produce well characterized metal-free diamond material.

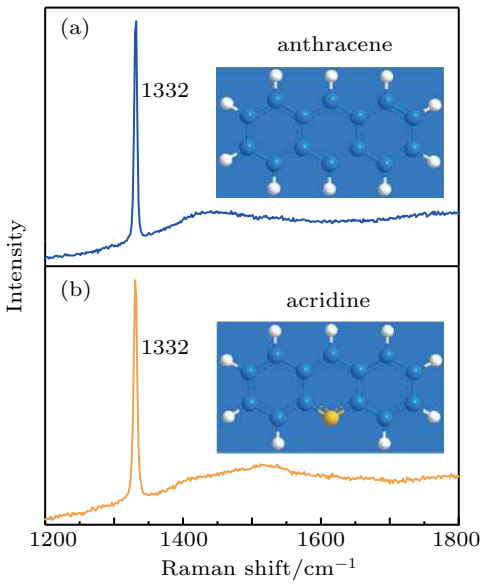

Fig. 6. Raman spectra of diamond obtained employing (a) anthracene and (b) acridine as precursors in the two-step HPHT method.

To investigate the versatility of the two-step HPHT method, anthracene and acridine were also employed as precursors for synthesizing diamonds. As shown in Fig. 6, the Raman peak at 1332 cm^{-1} reveals the formation of diamond in both cases. This indicates that the two-step HPHT process is a general method to prepare diamonds from other organic precursors.

4. Conclusion

A two-step HPHT method was used for the size-controlled synthesis of diamonds, employing naphthalene as a precursor without metal catalysts. The average grain size of the diamonds could be tuned by adjusting the carbonization time. This was attributed to the effect of carbon intermediates with different crystallinities on the nucleation and growth of the diamonds. This work provides an approach for tuning the grain size of diamonds and overcoming secondary anvil cracking, and can be applied to other organic precursors for producing nanodiamonds.

References

[1] Huang Q, Yu D L, Xu B, Hu W T, Ma Y M, Wang Y B, Zhao Z S, Wen B, He J L, Liu Z Y and Tian Y J 2014 *Nature* **510** 250
[2] Wen B, Xu B, Wang Y B, Gao G Y, Zhou X F, Zhao Z S and Tian Y J 2019 *npj. Comput. Mater.* **5** 117
[3] Hu W T, Wen B, Huang Q, Xiao J W, Yu D L, Wang Y B, Zhao Z S, He J L, Liu Z Y, Xu B and Tian Y J 2017 *Sci. Chin. Mater.* **60** 178
[4] Su L X, Lou Q, Zang J H, Shan C X and Gao Y F 2017 *Appl. Phys. Express* **10** 025102
[5] Mochalin V N, Shenderova O, Ho D and Gogotsi Y 2012 *Nat. Nanotechnol.* **7** 11
[6] Chu H Y, Hsu W C and Lin J F 2010 *Wear* **268** 960
[7] Lin W M, Kato T, Ohmori H and Osawa E 2009 *Key. Eng. Mater.* **404** 131
[8] Kurtsiefer C, Mayer S, Zarda P and Weinfurter H 2000 *Phys. Rev. Lett.* **85** 290

[9] Zhang H C, Chen C K, Mei Y S, Li X, Jiang M Y and Hu X J 2019 *Chin. Phys. B* **28** 076103
[10] Yang C, Wang X P, Wang L J, Pan X F, Li S K and Jing L W 2013 *Chin. Phys. B* **22** 088101
[11] Zhang D X, Zhao Q, Zang J H, Lu Y J, Dong L and Shan C X 2018 *Carbon* **127** 170
[12] Huang H J, Pierstorff E, Osawa E and Ho D 2007 *Nano Lett.* **7** 3305
[13] Zhang X Q Chen M, Lam R, Xu X Y, Osawa E and Ho D 2009 *ACS Nano* **3** 2609
[14] Qin S R, Zhao Q, Cheng Z G, Su L X and Shan C X 2018 *Acta Phys. Sin.* **67** 166801 (in Chinese)
[15] Moore L, Chow E K H, Osawa E, Bishop J M and Ho D 2013 *Adv. Mater.* **25** 3532
[16] Chang Y R, Lee H Y, Chen K, Chang C C, Tsai D S, Fu C C, Lim T S, Tzeng Y K, Fang C Y, Han C C, Chang H C and Fann W 2008 *Nat. Nanotechnol.* **3** 284
[17] Zhang X Q, Lam R, Xu X Y, Chow E K, Kim H J and Ho D 2011 *Adv. Mater.* **23** 4770
[18] Zhang K K, Zhao Q, Qin S R, Fu Y, Liu R Z, Zhi J F and Shan C X 2019 *J. Colloid Interf. Sci.* **537** 316
[19] Su L X, Lou Q, Jiao Z and Shan C X 2016 *Nanoscale Res. Lett.* **11** 425
[20] Khan M B and Khan Z H 2018 *Nanodiamonds: synthesis and applications* (Singapore: Springer Nature) p. 1
[21] Dong J J, Yao Z, Yao M G, Li R, Hu K, Zhu L Y, Wang Y, Sun H H, Sundqvist B, Yang K and Liu B B 2020 *Phys. Rev. Lett.* **124** 065701
[22] Osawa E 2005 *Disintegration and purification of crude aggregates of detonation nanodiamond: A few remarks on nano methodology* (Netherlands: Springer) p. 231
[23] Pichot V, Comet M, Fousson E, Baras C, Senger A, Normand F L and Spitzer D 2008 *Diam. Relat. Mater.* **17** 13
[24] Han F, Li S S, Jia X F, Chen W Q, Su T C, Hu M H, Yu K P, Wang J K, Wu Y M, Ma H A and Jia X P 2019 *Chin. Phys. B* **28** 028103
[25] Fan X H, Xu B, Niu Z, Zhai T G and Tian B 2012 *Chin. Phys. Lett.* **29** 048102
[26] Ekimov E A, Kudryavtsev O S, Mordvinova N E, Lebedev O I and Vlasov I I 2018 *ChemNanoMat.* **4** 269
[27] Konyashin I, Frost D J, Crossley A, Jurkschat K, Johnston C and Armstrong K 2016 *Mater. Lett.* **183** 14
[28] Davydov V A, Agafonov V and Khabashesku V N 2016 *J. Phys. Chem. C* **120** 29498
[29] Li Z, Zang J H, Lou Q, Yang X G, Dong B S, Liu T and Wang S L 2019 *Chin. J. Lumin.* **40** 153
[30] Smith E M and Wang W Y 2016 *Diam. Relat. Mater.* **68** 10
[31] Sokol G, Tomilenko A A, Bul'bak T A, Sokol L A, Persikov E S, Bukhtiyarov P G and Palyanov Y N 2018 *High Press. Res.* **38** 468
[32] Walker D, Carpenter M A and Hitch C M 1990 *Am. Miner.* **75** 1020
[33] Leinenweber K D, Tyburczy J A, Sharp T G, Soignard E, Diedrich T, Petuskey W B, Wang Y and Mosenfelder J L 2012 *Am. Miner.* **97** 353
[34] Angadi V J, Anupama A V, Kumar R, Choudhary H K, Matteppanavar S, Somashekarappa H M, Rudraswamy B and Sahoo B 2017 *Mater. Chem. Phys.* **199** 313
[35] Liang Y C, Liu K K, Lu Y J, Zhao Q and Shan C X 2018 *Chin. Phys. B* **27** 078102
[36] Shinohara H, Yamakita Y and Ohno K 1998 *J. Mol. Struct.* **442** 221
[37] Tan D Z, Zhou S F, Xu B B, Chen P, Shimotsuma Y, Miura K and Qiu J R 2013 *Carbon* **62** 374
[38] Franklin R E 1950 *Acta. Cryst.* **3** 107
[39] Kinoshita K 1988 *Carbon-electrochemical and physicochemical properties* (New York: John Wiley & Sons)
[40] Ferrari A C and Robertson J 2000 *Phys. Rev. B* **61** 14095
[41] Yang X G, Yao M G, Wu X Y, Liu S J, Chen S L, Yang K, Liu R, Cui T, Sundqvist B and Liu B B 2017 *Phys. Rev. Lett.* **118** 245701
[42] Chanyshev A D, Litasov K D, Furukawa Y, Kokh K A and Shatskiy A F 2017 *Sci. Rep.* **7** 7889
[43] Spanu L, Donadio D, Hohl D, Schwegler E and Galli G 2011 *Proc. Natl. Acad. Sci.* **108** 6843
[44] Fang S, Ma H A, Guo L S, Chen L C, Wang Y, Ding L Y, Cai Z H, Wang J and Jia X P 2019 *Chin. Phys. B* **28** 098101
[45] Yang X G, Lv C F, Yao Z, Yao M G, Qin J X, Li X, Shi L, Du M R, Liu B B and Shan C X 2020 *Carbon* **159** 266
[46] Higashi K and Onodera A 1986 *Physica B+C* **139** 813
[47] Onodera A, Higashi K and Irie Y 1988 *J. Mater. Sci.* **23** 422
[48] Onodera A, Irie Y and Higashi K 1991 *J. Appl. Phys.* **69** 2611
[49] Kamali A R and Fray D J 2015 *Chem. Commun.* **51** 5594
[50] Liu W Q, Ma H A, Li X L, Liang Z Z, Liu M L, Li R and Jia X P 2007 *Chin. Phys. Lett.* **24** 1749
[51] Guillou C L, Brunet F, Irifune T, Ohfuji H and Rouzaud J N 2007 *Carbon* **45** 636
[52] Khaliullin R Z, Eshet H, Kuhne T D, Behler J and Parrinello M 2011 *Nat. Mater.* **10** 693
[53] Li Y D, Chen Y S, Su M J, Ran Q F, Wang C X, Ma H A, Fang C and Chen L C 2020 *Chin. Phys. B* **29** 078101